Heavy resonances and top production Overview of top tagging techniques

José Juknevich

Weizmann Institute of Science, Rehovot, 76100 Israel &
SISSA, I-34136 Trieste, Italy

DOI: http://dx.doi.org/10.3204/DESY-PROC-2014-02/35

Events containing hadronically decaying top quarks with large momentum are playing an increasingly significant role, both in searches for new physics and measurements of Standard Model processes at the Large Hadron Collider. Such events are not fully described by traditional reconstruction techniques, because boosted top decays are very collimated, leading to merged jet topologies. We review top tagging techniques that can contribute to the identification of boosted top jets. We also point out some issues that may arise in searches that make use of such substructure information.

1 Introduction

The study of substructure of boosted massive jets gives insight into the fundamental structure of QCD and an opportunity to tune the various Monte Carlo (MC) event generators. These exotic jets are also becoming increasingly important at the Large Hadron Collider (LHC), with the experimental searches entering a kinematic regime in which a significant fraction of heavy Standard Model (SM) particles are produced at high transverse momentum (p_T). Of particular interest are boosted top quarks, as many models of new physics that address the hierarchy problem predict states with a large decay rate to top quark pairs (see for example Refs. [1, 2, 3, 4, 5, 6, 7]).

At high p_T, the decay products of heavy objects tend to be collimated in the lab frame and are not adequately described by standard reconstruction techniques. As a rule of thumb, one can estimate the opening angle of decay products of a boosted object as $\Delta R \gtrsim 2M/p_T$, where M is the mass of the decaying resonance (top or W) and p_T its transverse momentum. Consequently, by using usual jets with a radius $R = 0.4$ or $R = 0.5$, the decay products of the W in $t \to bW \to bq\bar{q}$ may not be resolved if $p_T^W \gtrsim 300\,\text{GeV}$. Using smaller R to directly resolve the subjets results in significant loss of gluon radiation from the $W \to q\bar{q}$ system, giving poor mass resolution.

An alternative method is to cluster the resulting hadrons into "fat jets" with large radius parameter ($R = 1.0$ or $R = 1.5$), in order to collect all decay products [8, 9, 10]. This gives us the flexibility to solve some combinatorial issues while also ensuring the capture of interesting gluon radiation from decay products. The leading order (LO) three prong decay structure of a boosted top and the correlations therein can be employed to distinguish top quark jets from, say, light parton QCD jets, which typically have a two prong topology. Many different approaches have been developed to exploit these differences and will be the focus of this review.

2 Jets and jet substructure

Understanding jets and why they are important phenomenological tools is a critical step to understand jet substructure and its applications. Jets are the objects that enable us to connect long-distance effects with perturbatively describable short-distance physics. The property of QCD that allows this is called factorization. It can be used to write hard scattering cross-sections as convolutions of separate hard, jet, and soft functions. The soft and jet functions are the only ones that are associated to the particular jet and its definition. Reasonable calculations of these functions can be carried out in the limit of small jet radius R. This allows us to consider only contributions from the jet functions, which are related to radiation from the parton that originated the jet, and ignore the soft functions, which depend on large-angle radiation from other final-state partons and from the initial-state partons.

2.1 Sequential recombination algorithms

Jets, however, are not unambiguous objects. To be able to compare experimental observations to theoretical predictions, jets have to be defined in an infrared safe way, i.e. insensitive to the emission of soft or collinear particles. This is because the QCD matrix elements have singularities whenever a soft gluon or collinear pair of massless partons is emitted. Many jet clustering algorithms have been proposed for the analysis of hadronic final states in hadron-hadron collisions. Of course, when comparing experiment with theory, it is important to use the same algorithm to ensure consistency in the results.

Some of the jet algorithms that are in widespread use at the LHC are sequential recombination algorithms. Here jets are constructed by iteratively recombining final state particles pairwise according to some measure d_{ij}. The three most popular sequential jet algorithms are the k_T [11], the Cambridge/Aachen (CA) [12] and the anti-k_T [13] algorithms. Their measure is given by

$$d_{ij} = \min(p_{T,i}^{2p}, p_{T,j}^{2p})\frac{\Delta R_{ij}^2}{R^2} \qquad d_{iB} = p_{T,i}^{2p}, \tag{1}$$

where $p = 1, 0, -1$ for the k_T, CA and anti-k_T algorithms, respectively, and R is the jet resolution parameter. These algorithms sequentially merge the pair of protojets (by combining their four vectors) which are closest according to d_{ij}, unless one of the d_{iB} is smaller than all d_{ij}, in which case the protojet i is deemed a jet and the procedure continues on the remaining objects.

The choice of jet algorithm and resolution parameter R depends on the topology and experimental context of interest. A jet algorithm may be preferred because of its larger background rejection rate, insensitivity to contamination, or, as we will se below, because it is able to highlight certain aspects of the substructure of jets. Determining an optimal jet radius R is a compromise between taking it large enough to catch the bulk of gluon radiation and small enough to avoid too much contamination from the underlying event (UE) and pileup. ATLAS and CMS have many different jet finding algorithms and choices of jet radii, ensuring some degree of flexibility at the time of performing an analysis.

2.2 The importance of jet mass

While looking for a resonance massive jet, the jet mass is a good indicator of its origin. Assuming a given jet p_T, and working in the collinear regime (small R), the leading-order differential QCD jet-mass distribution is given by [16, 17]

$$\frac{1}{\sigma}\frac{d\sigma}{dm_J^2} \approx \frac{\alpha_s C_F^2}{\pi m_J^2}\left(\ln\frac{R^2 p_T^2}{m_J^2} + \mathcal{O}(R^2)\right) \tag{2}$$

where C_F are the color factors associated with the representation of the particle initiating the jet. In the region of interest for boosted object studies, $m_J \ll p_T$, the logarithmic term in Eq. (2) can be large even when electroweak scale jet masses are considered. An accurate description of massive jets therefore requires to consider variables that can resolve finer details of the substructure of jets, beyond the jet mass and p_T.

Subjet techniques aim to identify relatively hard, symmetric splittings which are most likely associated to a heavy particle decay. In the leading log approximation, we can describe a massive jet composed of two subjets by

$$\frac{m_J^2}{p_{T,J}^2} \sim z(1-z)\Delta R^2_{j_1 j_2}, \qquad \text{with } z = \frac{\min p_{T,j_i}}{p_{T,J}}. \tag{3}$$

If one of these splittings corresponds to $t \to bW$ or $W \to jj$, we expect symmetric decays with $z \sim 0.5$. For a given mass, QCD subjets also tend to be symmetric but much less so, owing to the different nature of the splittings. This provides us a way of placing cuts on the z fractions, so as to eliminate backgrounds. Once a small angular scale $\Delta R_{j_1 j_2}$ has been found, it can be used for resolving the jet at a even smaller scale to remove soft radiation and further improve on jet mass resolution.

2.3 Jet grooming

At the large luminosities present at the LHC, additional energy depositions from the UE, pileup or initial state radiation may hinder substructure studies. These additional contributions are uncorrelated with the hard-scattering process that originated the event and introduce a background of soft diffuse radiation. The soft diffuse pileup/UE background can have a large impact on the jet mass, p_T and other jet substructure observables, especially for large-R jets. It is thus important that measurements of jet substructure be able to remove this extra energy from the reconstructed jets.

Several grooming techniques are available to mitigate the effects of pile-up and UE. The purpose of these methods is to remove particles in a jet which are most likely associated with uncorrelated sources of radiation. The most commonly used grooming techniques are filtering [8], trimming [14] and grooming [15]. Jet filtering and trimming work in a similar fashion by re-clustering the constituents of a fat jet using a k_T jet algorithm with smaller radius $R_{\rm sub}$ to find subjets of the original jet. Only a subset of these subjets is kept. Filtering keeps a fixed number n_f of subjets. Trimming, instead, keeps only the subjets which satisfy $p_{T,i} > f_{\rm cut} \times p_T^{\rm jet}$, where $f_{\rm cut}$ is an adjustable parameter.

Likewise, pruning tries to clean jets from soft and wide angle radiation. Unlike the case of filtering and trimming, pruning works instead by discarding particles at each recombination step of a k_T or CA jet algorithm. At each recombination step $ij \to a$, the algorithm checks for either two conditions,

$$z = \frac{\min(p_{T,i},\, p_{T,j})}{|\vec{p}_{T,i} + \vec{p}_{T,j}|} < z_{\rm cut}, \qquad \Delta R_{ij} > D_{\rm cut}, \tag{4}$$

where $z_{\rm cut}$ and $D_{\rm cut}$ are two parameters that have to be optimized for each process of interest. If both conditions are met then one drops the softer of i, j, and continues the process. The algorithm continues until all constituents have either been combined or else removed.

It has been shown that grooming techniques improve the jet's mass resolution [18]. This property can be used to increase the sensitivity of a resonance search. One should only be aware that the cuts are placed on infrared safe observables, so as not to spoil the infrared safety properties of the original, ungroomed jets.

3 Techniques to reconstruct boosted top jets

In this Section we present a very brief overview of some of the most popular top tagging techniques, focusing on the ones that are already in use by the LHC experiments. These methods can be grouped into two broad categories. The first class includes methods that characterize signal events by subjets that would correspond to the decay of heavy particles. The second class employs jet shape observables to probe the energy radiation pattern within jets. The choice of a top tagger is a compromise between maintaining a high signal efficiency or delivering a large background rejection. Thus, the question of which top tagger is the "best" depends on the search or measurement in question.

3.1 k_t splitting scales, d_{ij}

One widely used class of substructure observables are the splitting scales in the last stages of jet clustering by a k_T jet algorithm. They were applied by ATLAS in combination with jet mass as a simple way of tagging tops [19]. The method is optimized to work at larger tagging efficiencies, where basic event selections already remove a large fraction of the background. The k_T distance of the final clustering step defines a splitting variable $\sqrt{d_{12}}$:

$$\sqrt{d_{12}} = \min{(p_{T,j_1}, p_{T,j_2})} \Delta R_{j_1 j_2}, \tag{5}$$

Similarly, one can define a splitting scale $\sqrt{d_{23}}$ of the next-to-final clustering step. The ordering of clustering in the k_T algorithm implies that decay products of massive particles are typically combined in the last steps of recombination. Thus, one expects $\sqrt{d_{12}} \approx m_t/2$ and $\sqrt{d_{23}} \approx m_W/2$ for a fat jet containing all top decay products $t \to bW \to bq\bar{q}$, while QCD jets typically give much smaller splittings.

3.2 John Hopkins top tagger

The "Hopkins" top tagger [20] is inspired by the BDRS algorithm [8] applied to boosted Higgs identification. The fat jet is found using the CA algorithm with $R = 0.8$. This jet is then decomposed by reversing the clustering history, iteratively splitting each jet into two objects $j \to j_1 + j_2$. The softer of the two objets is thrown out if $\min p_{T,j_i} < \delta_P p_T^{\rm jet}$, for some parameter δ_P, and the procedure continues on the harder objects. The declustering step is repeated until an interesting splitting is found such that

$$\Delta R_{j_1 j_2} > \delta_R, \qquad \min p_{T,j_i} > \delta_P \, p_T^{\rm jet}, \tag{6}$$

where δ_R is an additional parameter. The next step is to successively uncluster both j_1 and j_2 to find jets with 3 or 4 subjets. If the resulting subjets satisfy several kinematical constraints consistent with a boosted top decay (e.g. the total invariant mass of all subjets should be near m_t, two of the subjets are required to reconstruct m_W and their helicity angle should not be too small,) the jet is deemed a top candidate. The "Hopkins" top tagger has been modified by CMS [21], where the kinematic cuts have been replaced by a single cut on the minimum pairwise subjet mass.

3.3 HEPtopTagger

Similarly to the John Hopkins tagger, the HEPTopTagger [22, 23] is another tagger inspired by the BDRS method. It was originally designed to efficiently identify mildly-boosted top jets, with $p_T \gtrsim 200\,\text{GeV}$. The algorithm begins by clustering the event using a CA algorithm with an extremely large angular scale $R = 1.5$, and requiring the jet to have $p_T > 200\,\text{GeV}$. The next step is to iteratively uncluster the jet while looking for some interesting substructure. The criterion for an interesting splitting $j \to j_1 j_2$ is that the subjets must satisfy a mass drop condition $m_{j_i} < 0.2 m_j$. If the splitting fails this criterion, the lightest subjet is discarded and the procedure continues recursively on the heavier object. The procedure ends when all the subjets satisfy $m_{j_i} < 30\,\text{GeV}$. The next step is to apply jet filtering on the constituents of the surviving subjet's $\{j_i\}$, with a small angular resolution scale $R_{filt} = \min(0.3, \Delta R_{ij})$, and retain five subjets. This step is performed in order to reduce sensitivity to pileup/UE. These five filtered subjets are then once more reclustered into exactly three subjets, which are the candidates for the top decay products. Finally, the invariant mass combinations of the three subjets are reconsidered in the $(m_{23}/m_{123},\, \arctan(m_{13}/m_{12}))$ plane. For tops, one of the combinations is required to satisfy,

$$0.85\frac{m_W}{m_t} \lesssim \frac{m_{23}}{m_{123}} \lesssim 1.15\frac{m_W}{m_t}, \qquad 0.2 \lesssim \arctan\frac{m_{13}}{m_{12}} \lesssim 1.3. \tag{7}$$

These kinematic cuts pick out top jets, while the background is typically concentrated on small pairwise invariant masses.

3.4 Template Overlap Method

The Template Overlap Method [24] differs from the above approaches in that it does not manipulate the jet constituent list, nor does it require a special clustering algorithm for substructure analysis. Instead, the method compares the jet to a set of parton level states built according to a fixed-order distribution of signal jets called templates. The comparison makes use of an "overlap function" which evaluates the level of agreement between each measured jet and a set of templates.

Let us consider the case of a boosted top quark decay $t \to bW \to bq\bar{q}$. The phase space for this decay is determined by four independent parameters, which can be chosen as the rapidity and azimuthal angle of the W decay daughters, $(\eta, \phi)_{i=1,2}$ in the lab frame. Each top template consists of a set of three momenta (p_1, p_2, p_3) at fixed total p_T obtained by sequentially scanning over the phase space given by the above four angular variables.

Following the notation of Ref. [25], here we consider the definition of *hadronic peak template overlap* in terms of longitudinally boost invariant quantities:

$$Ov_3 = \max_{\{f\}} \left\{ \exp\left[-\sum_{a=1}^{N} \frac{1}{\sigma_a^2} \left(\epsilon\, p_{T,a} - \sum_{\Delta R(i,a) < r_a} p_{T,i} \right)^2 \right] \right\}, \tag{8}$$

where $p_{T,a}$ is the transverse momentum of the a^{th} template parton and $p_{T,i}$ is the transverse momentum of the i^{th} jet constituent. The functional is maximized over the set of templates f constructed by the above procedure. The weight σ_a defines the energy resolution of the peak template overlap which we set to $\frac{1}{3}p_{T,a}$, while the coefficient ϵ serves to compensate for the radiation which falls outside the template sub-cones.

It has been shown that Ov_3 is a good discriminant between top jets and QCD light parton jets [24, 26]. In addition, placing limits on the distributions of the best matched templates gives additional information on the likelihood that the jet is signal or background. The template-based observables by themselves are robust against pileup up to 50 interactions per bunch crossing, without the use of additional pileup correction techniques [25, 26]. The relative insensitivity of the Template Overlap Method to pileup may thus serve to study the systematic effects of other pileup correction techniques.

3.5 Other top tagging approaches

Methods that employ a different approach to probing the substructure of jets also exist. The jet observable N-subjettiness [27, 28] is designed to classify jets as being N-prong-like without any reference to jet algorithms. Given N axes $\hat{n}_i$, N-subjettiness is defined by

$$\tau_N = \frac{1}{d_0} \sum_{k \in J} p_{T,k} \min\{\Delta R_{1,k} \cdots \Delta R_{N,k}\}, \quad (9)$$

with

$$d_0 = \sum_{k \in J} p_{T,k} R_0. \quad (10)$$

Here the index k runs over all the jet's constituents. τ_N measures the extent to which the N-subjet description provides a good characterization of the energy distribution within jets. This provides an useful handle to disentangle heavy-object jets from light parton QCD jets. It was shown that the real discrimination power of N-subjettiness occurs when considering ratios of N-subjettiness, $r_N = \tau_N/\tau_{N-1}$. For heavy particles with N-prong decays, r_N is expected to peak at larger values compared to the QCD case. One should be aware that these ratios by themselves are not infrared and collinear safe for generic jets. In particular, r_N is infrared safe only when applied to jets with a N-prong substructure, which can be guaranteed through a cut on r_{N-1}. A simple top tagger can be constructed using as input variables the jet mass, τ_2/τ_1 and τ_3/τ_2.

More recently, shower deconstruction method [29, 30] appeared as a variant of the matrix element method to classify jets with the help of approximations to hard matrix elements and the parton shower. The method attempts to identify boosted hadronic tops by computing the ratio of the likelihood for a jet to have been originated from a top decay to the likelihood for the same jet to have been originated from a light QCD parton. These likelihoods are computed by summing over all possible shower histories leading to the observed final state, using first principle QCD, in a similar fashion to what full event generators do. The results presented in Ref. [30] show an improvement on the top taggers described previously.

4 Asymmetric $t\bar{t}$ production from higher-order amplitudes

The first area where top tagging has proved fruitful is in searches for new physics decaying to top quark pairs. The $t\bar{t}$ topologies we observed in the detector depend strongly on the kinematic regime, as quantified by the H_T of the event (here we define $H_T = \sum_j p_{T,j}$, where j runs over all final state particles in the event.) Low-energy events, the top and anti-top are produced nearly back to back with about the same p_T. Yet, high energy events often involve extra hard radiation in the final state as well as a non-negligible gluon splitting function to heavy flavors, all of which can result in an imbalance between the transverse momenta of the top and anti-top [26, 31]. The contributions from these categories of events are depicted in Fig. 1.

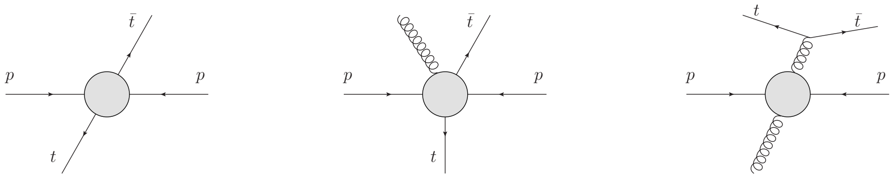

(i) (ii) (iii)

Figure 1: Three categories of $t\bar{t}$ events. Figure from Ref. [26].

Contributions from asymmetric events belonging to class (ii) and (iii) in the SM $t\bar{t}$ production are of great importance to measure the SM top differential p_T distribution. However, including these asymmetric events into the event sample might cause the gluon jet to be misidentified as the hadronic top, and an inaccurate reconstruction of the event. On the other hand, the rejection of asymmetric events is of particular relevance in searches for new physics. For instance, top quark pairs produced in heavy resonance decays typically belong to class (i). Hence, rejecting asymmetric events implies that the SM $t\bar{t}$ is not an irreducible background anymore and a further improvement in signal to background can be achieved. All of this stresses the importance of using a good top tagger, with relatively high efficiency and better background rejection.

Acknowledgments

It is a pleasure to thank U. Husemann and the organizers for the opportunity to be part of such an excellent workshop. I thank G. Perez for introducing me to jet substructure, and for many useful conversations during the course of our collaborations.

References

[1] R. M. Harris, C. T. Hill and S. J. Parke, hep-ph/9911288.

[2] C. T. Hill and S. J. Parke, Phys. Rev. D **49** (1994) 4454, hep-ph/9312324.

[3] K. Agashe, A. Belyaev, T. Krupovnickas, G. Perez and J. Virzi, Phys. Rev. D **77** (2008) 015003, hep-ph/0612015.

[4] B. Lillie, J. Shu and T. M. P. Tait, Phys. Rev. D **76** (2007) 115016, arXiv:0706.3960 [hep-ph].

[5] B. Lillie, L. Randall and L. -T. Wang, JHEP **0709** (2007) 074, hep-ph/0701166.

[6] R. Contino and G. Servant, JHEP **0806** (2008) 026, arXiv:0801.1679 [hep-ph].

[7] R. Contino, L. Da Rold and A. Pomarol, Phys. Rev. D **75** (2007) 055014, hep-ph/0612048.

[8] J. M. Butterworth, A. R. Davison, M. Rubin and G. P. Salam, Phys. Rev. Lett. **100** (2008) 242001, arXiv:0802.2470 [hep-ph].

[9] M. H. Seymour, Z. Phys. C **62** (1994) 127.

[10] J. M. Butterworth, B. E. Cox and J. R. Forshaw, Phys. Rev. D **65** (2002) 096014, hep-ph/0201098.

[11] S. Catani, Y. L. Dokshitzer, M. H. Seymour and B. R. Webber, Nucl. Phys. B **406** (1993) 187.

[12] S. Catani, Y. L. Dokshitzer, M. Olsson, G. Turnock and B. R. Webber, Phys. Lett. B **269** (1991) 432.

[13] M. Cacciari, G. P. Salam and G. Soyez, JHEP **0804** (2008) 063, arXiv:0802.1189 [hep-ph].

[14] D. Krohn, J. Thaler and L. -T. Wang, JHEP **1002** (2010) 084, arXiv:0912.1342 [hep-ph].

[15] S. D. Ellis, C. K. Vermilion and J. R. Walsh, Phys. Rev. D **81** (2010) 094023, arXiv:0912.0033 [hep-ph].

[16] L. G. Almeida, S. J. Lee, G. Perez, G. F. Sterman, I. Sung and J. Virzi, Phys. Rev. D **79** (2009) 074017, arXiv:0807.0234 [hep-ph].

[17] M. Dasgupta, K. Khelifa-Kerfa, S. Marzani and M. Spannowsky, JHEP **1210** (2012) 126, arXiv:1207.1640 [hep-ph].

[18] A. Abdesselam, E. B. Kuutmann, U. Bitenc, G. Brooijmans, J. Butterworth, P. Bruckman de Renstrom, D. Buarque Franzosi and R. Buckingham *et al.*, Eur. Phys. J. C **71** (2011) 1661, arXiv:1012.5412 [hep-ph].

[19] G. Aad *et al.* [ATLAS Collaboration], Phys. Rev. D **86** (2012) 072006, arXiv:1206.5369 [hep-ex].

[20] D. E. Kaplan, K. Rehermann, M. D. Schwartz and B. Tweedie, Phys. Rev. Lett. **101**, 142001 (2008), arXiv:0806.0848 [hep-ph].

[21] [CMS Collaboration], CMS-PAS-JME-09-001.

[22] T. Plehn, M. Spannowsky and M. Takeuchi, Phys. Rev. D **85** (2012) 034029, arXiv:1111.5034 [hep-ph].

[23] T. Plehn, G. P. Salam and M. Spannowsky, Phys. Rev. Lett. **104** (2010) 111801, arXiv:0910.5472 [hep-ph].

[24] L. G. Almeida, S. J. Lee, G. Perez, G. Sterman and I. Sung, Phys. Rev. D **82** (2010) 054034, arXiv:1006.2035 [hep-ph].

[25] M. Backovic, J. Juknevich and G. Perez, JHEP **1307** (2013) 114, arXiv:1212.2977 [hep-ph].

[26] M. Backovic, O. Gabizon, J. Juknevich, G. Perez and Y. Soreq, arXiv:1311.2962 [hep-ph].

[27] J. Thaler and K. Van Tilburg, JHEP **1103** (2011) 015, arXiv:1011.2268 [hep-ph].

[28] J. Thaler and K. Van Tilburg, JHEP **1202** (2012) 093, arXiv:1108.2701 [hep-ph].

[29] D. E. Soper and M. Spannowsky, Phys. Rev. D **84** (2011) 074002, arXiv:1102.3480 [hep-ph].

[30] D. E. Soper and M. Spannowsky, Phys. Rev. D **87** (2013) 054012, arXiv:1211.3140 [hep-ph].

[31] G. Salam, http://www.lpthe.jussieu.fr/∼salam/talks/repo/2013-Top4ATLAS-Top4ATLAS.pdf.